

**Composition and thermal-annealing-induced short-range ordering changes
in amorphous hydrogenated silicon carbide films as investigated
by extended x-ray-absorption fine structure and infrared absorption**

M. A. El Khakani, D. Guay, and M. Chaker

*Institut National de la Recherche Scientifique—Énergie et Matériaux, 1650 Montée Ste-Julie, Case Postale 1020,
Varenes, Québec, Canada J3X 1S2*

X. H. Feng

Department of Chemistry, University of Western Ontario, London, Ontario, Canada N6A 3K7

(Received 29 June 1994)

We have studied the effect of the film composition and the post-annealing treatment on both the first-shell local structure around the Si atoms and the bonding states of amorphous hydrogenated silicon carbide films ($a\text{-Si}_x\text{C}_{1-x}\text{:H}$), prepared by the plasma-enhanced chemical-vapor-deposition technique. The local structure was characterized by measuring the extended x-ray-absorption fine structure at the Si K edge, whereas the Si-H, C-H, and Si-C bond densities were determined by using Fourier-transform infrared spectroscopy. The Si/C atomic ratio and the total hydrogen content were measured by means of the elastic-recoil-detection nuclear method. We have found that the Si-C and Si-Si bond lengths in the first coordination shell are, respectively, 1.88 and 2.35 Å, and are independent of both the film composition and the annealing temperature. Taking into account the presence of Si-H and C-H hydrogenated bonds, we have obtained both qualitative and quantitative analyses of the short-range order changes, as a function of (i) the composition of $a\text{-Si}_x\text{C}_{1-x}\text{:H}$ ($0.26 \leq x \leq 0.91$) alloys, and (ii) the annealing temperature ($300^\circ\text{C} \leq T \leq 850^\circ\text{C}$) of $a\text{-SiC:H}$ films ($x=0.5$). The type of local disorder in the films was determined by calculating their corresponding short-range-order coefficients ($\eta_{\text{Si,C}}^0$), by means of a theoretical model. We were thus able to show that, depending on the film composition, the short-range order is characterized either by a chemical preference for Si-C nearest-neighbor pairs (for $0.26 \leq x \leq 0.55$) or by chemical clustering that favors the formation of Si-Si bonds in the local Si environments (for $x \geq 0.77$). On the other hand, we show that thermal annealings of $a\text{-SiC:H}$ films cause partial dissociation of hydrogenated bonds (Si-H and C-H), which results in evacuation of hydrogen atoms and additional Si-C bond formation. These microstructural rearrangements are enhanced as the annealing temperature is increased beyond 650°C , and occur with a strong local chemical ordering that favors the formation of Si-C bonds. Concomitantly the stress of $a\text{-SiC:H}$ films varies from highly compressive (-1 GPa) to highly tensile ($+1$ GPa), as the annealing temperature is increased from 300 to 850°C . Finally, we show that this stress variation of $a\text{-SiC:H}$ films correlates well with the variations of their partial coordination numbers, their bond densities, and their degree of structural disorder.

I. INTRODUCTION

Amorphous hydrogenated silicon carbide ($a\text{-Si}_x\text{C}_{1-x}\text{:H}$) alloys continue to attract great interest from both fundamental and application viewpoints. Due to their unique optical, electrical and mechanical properties, $a\text{-Si}_x\text{C}_{1-x}\text{:H}$ films cover a wide range of potential applications, such as solar cells,¹ optoelectronic devices,²⁻⁴ high-temperature engineering materials,⁵ coating materials for biocompatible implants,⁶ and x-ray membranes for x-ray lithography.^{7,8} The properties of these alloys generally depend on their structure and composition, allowing their tailoring with optimized properties for a given application.^{9,10}

On the other hand, $a\text{-Si}_x\text{C}_{1-x}\text{:H}$ alloys constitute a challenging material for fundamental studies of an amorphous ternary alloy with a complex disorder and variable microstructure. $a\text{-Si}_x\text{C}_{1-x}\text{:H}$ alloys are expected to be the most disordered semiconducting alloys as compared

to $a\text{-Si:H}$, $a\text{-Si}_x\text{Ge}_{1-x}\text{:H}$, and $a\text{-Si}_x\text{N}_{1-x}\text{:H}$ alloys.^{1,11} Indeed, in addition to the chemical disorder, the structural disorder is enhanced because of (i) the various coordination geometries as a result of differences in Si-Si, Si-C, Si-H, C-H, and C-C bonds lengths, and the different covalent radii of silicon and carbon atoms (in contrast to silicon and germanium atoms having basically the same covalent radii¹); (ii) the possibility of formation of homonuclear carbon bonds with various hybridizations (sp , sp^2 , and sp^3); and (iii) the presence of Si-H and C-H hydrogenated bonds, which induce a high compressive stress in the as-deposited $a\text{-Si}_x\text{C}_{1-x}\text{:H}$ films.¹² Their dissociation, under the effect of high-temperature ($> 600^\circ\text{C}$) annealings, leads to an increase of the structural disorder.¹³

So far, plasma-enhanced chemical-vapor deposition (PECVD) by rf glow discharge decomposition of silane and a hydrocarbon gas (often, methane), is the most widely used method for preparing $a\text{-Si}_x\text{C}_{1-x}\text{:H}$ films. These

deposited films have been the subject of numerous microstructural investigations using various analysis techniques.^{9,11,14-18} Although the microstructure of $a\text{-Si}_x\text{C}_{1-x}\text{:H}$ films closely depend on the deposition conditions,^{1,19} it arises from these studies that $a\text{-Si}_x\text{C}_{1-x}\text{:H}$ films present a macroscopic homogeneous but a microscopic heterogeneous structure characterized by various local environments. Proposed approaches for investigating these $a\text{-Si}_x\text{C}_{1-x}\text{:H}$ alloys range from the model (initially developed from Si-H band infrared-absorption studies,^{14,15}), which simply describes silicon carbide films as a tetrahedral network where the C and Si atoms are randomly distributed and where only one single hydrogen is bonded to each silicon, to those of recent works showing that hydrogenated amorphous silicon carbide films are microscopically heterogeneous with evidence for homogeneous or partial chemical ordering promoting heteroatomic bonds in local environments.¹⁶ Few investigations of the first coordination shell of Si atoms in $a\text{-Si}_x\text{C}_{1-x}\text{:H}$ alloys as a function of the film composition have been also performed by means of extended x-ray-absorption fine-structure (EXAFS) spectroscopy.²⁰⁻²⁴ These studies revealed the presence of a tendency to local chemical ordering,^{21,22} especially for $a\text{-Si}_x\text{C}_{1-x}\text{:H}$ films with $x \leq 0.5$.²⁴ However, in most cases, the first-shell local structure was analyzed without taking into account the presence of hydrogenated bonds (Si-H and C-H) in $a\text{-Si}_x\text{C}_{1-x}\text{:H}$ films. More recently, a step in the theoretical studies of the microstructure of amorphous SiC films was crossed by using *ab initio* molecular dynamics simulations.²⁵ Although only the nonhydrogenated and stoichiometric SiC amorphous alloy has been considered, the picture obtained for $a\text{-SiC}$ alloy is rather complex and can be summarized as follows:²⁵ (i) about 40% of the bonds formed by C atoms are homonuclear, (ii) C atoms form bonds under both sp^2 and sp^3 hybridizations, and (iii) Si atoms form Si-C and Si-Si bonds, where Si gives rise to strongly distorted tetrahedral sites.

In this context, it is of particular interest to investigate further the microstructure of these $a\text{-Si}_x\text{C}_{1-x}\text{:H}$ alloys to answer many still open fundamental questions, such as the predominant form of disorder, as a function of the film composition, while considering the effect of hydrogenated bonds on the local disorder, and the characterization of the short-range-order changes when the hydrogenated bonds are dissociated under thermal annealings. To this end, we have combined three techniques: (i) EXAFS spectroscopy at the Si *K* absorption edge [a unique probe capable of providing local pictures (bond lengths and partial coordination numbers of Si-Si and Si-C bonds) of the surroundings of the absorbing Si atoms]; (ii) Fourier-transform infrared (FTIR) spectroscopy; and (iii) elastic-recoil-detection (ERD) nuclear method. These latter two techniques allow the characterization of the Si-H, C-H, and Si-C IR absorption bands and the determination of both the Si/C atomic ratio and the total hydrogen content, respectively. The combination of these complementary methods has allowed us the achievement of a detailed study of the first-shell local structure while considering the presence of hydrogenated bonds, in $a\text{-Si}_x\text{C}_{1-x}\text{:H}$ alloys.

The aim of this paper is threefold: (i) to determine the predominant form of local disorder that best describes $a\text{-Si}_x\text{C}_{1-x}\text{:H}$ films as a function of their composition; (ii) to determine the short-range ordering changes induced by thermal annealings of $a\text{-SiC:H}$ films, and point out the role of hydrogenated bonds (Si-H and C-H) in the thermal-annealing-induced stress variation (from highly compressive to highly tensile) of $a\text{-SiC:H}$ films; and (iii) to correlate this stress variation to both the bonding state changes and the degree of structural disorder of $a\text{-SiC:H}$ films. Thus, in Sec. III, we first discuss our results on the first-shell local structure of the Si atoms in $a\text{-Si}_x\text{C}_{1-x}\text{:H}$ films as a function of the film composition. Second, we report a study of the Si local environments changes in $a\text{-SiC:H}$ stoichiometric films annealed from 300°C up to 850°C. Finally, we discuss the correlation of the stress of $a\text{-SiC:H}$ films with their bonding states and degree of structural disorder. In Sec. IV, we present a quantitative characterization of the type of local disorder of the $a\text{-Si}_x\text{C}_{1-x}\text{:H}$ films, by means of a theoretical model,²⁶ that allows the calculation of the corresponding short-range-order coefficient ($\eta_{\text{Si-C}}^0$). For both film composition and annealing temperature parameters, a detailed characterization of the short-range order of $a\text{-Si}_x\text{C}_{1-x}\text{:H}$ alloys is achieved, while taking into account the ratio of hydrogenated bonds in the local environments.

II. EXPERIMENTAL AND EXAFS DATA ANALYSIS

The $a\text{-Si}_x\text{C}_{1-x}\text{:H}$ films were prepared by rf glow-discharge decomposition of silane and methane in a PECVD reactor using argon as a gas carrier.²⁷ They were deposited on undoped, double side-polished and (100) oriented 500- μm -thick silicon wafers of 3-in. diameter at a substrate temperature of about 250°C. The total gas pressure was 0.2 Torr. The rf power density at 100 kHz was approximately 0.3 W/cm². At this power density,¹⁹ decomposition of both methane and silane occurs and allows the deposition of $a\text{-Si}_x\text{C}_{1-x}\text{:H}$ films with any composition ($0 \leq x \leq 1$). The composition of the film can be controlled by varying the reactive gas flow ratio [$g = \text{SiH}_4/(\text{SiH}_4 + \text{CH}_4)$].²⁷ The deposition rate of $a\text{-Si}_x\text{C}_{1-x}\text{:H}$ films increases with g . Stoichiometric films ($x = 0.5$) are deposited at $g = 0.3$ and at a deposition rate of about 1 $\mu\text{m}/\text{h}$. Films with thicknesses ranging from 1 to 2 μm were studied. The $a\text{-Si}_x\text{C}_{1-x}\text{:H}$ films density varies from 2.2 g/cm³ for C-rich films ($x = 0.25$) to 2.4 g/cm³ for Si-rich films ($x = 0.8$), with a maximum value of about 2.5 g/cm³ around $x = 0.5$ composition.²⁷ The incorporation of the hydrogen into the deposited $a\text{-Si}_x\text{C}_{1-x}\text{:H}$ films is inherent to the PECVD deposition process when the deposition temperature is lower than 800°C. Depending on the film composition, and under the above-mentioned operating conditions, the hydrogen content of $a\text{-Si}_x\text{C}_{1-x}\text{:H}$ films can reach a value of 29 at. %, as determined by ERD analysis.

The as-deposited $a\text{-SiC:H}$ films are under a high compressive stress (-1 GPa). The film stress was determined by measuring the net radius of curvature of the coated Si wafer.¹² By using the rapid thermal annealing

technique, the film stress was varied from -1 GPa compressive to $+1$ GPa tensile when the temperature is increased from 300°C and 850°C . The $2\text{-}\mu\text{m}$ -thick $a\text{-Si}_x\text{C}_{1-x}\text{:H}$ films were isochronally annealed for 60 sec at temperatures ranging from 300°C to 850°C in steps of 50°C under a $[\text{N}_2 (90\%)/\text{H}_2 (10\%)]$ gas flow.

The Si-C, Si-H, and C-H infrared absorption bands were characterized by FTIR spectroscopy using a FTIR-BOMEM DA316 spectrometer in the $(400\text{--}4000)\text{ cm}^{-1}$ spectral region.¹² Using the oscillator strengths^{28,29} and the integrated absorbances of Si-C, Si-H, and C-H stretching bands (peaking around 780 , 2100 , and 2900 cm^{-1} , respectively), the corresponding Si-C, Si-H, and C-H bonds densities were estimated.^{12,18}

The ERD nuclear method was used to depth profile hydrogen, silicon, and carbon elements in $a\text{-Si}_x\text{C}_{1-x}\text{:H}$ films. Consequently, the Si/C atomic ratio and the total hydrogen content of the films were precisely determined. The ERD experiments were performed using a ^{35}Cl beam of 30 MeV incident energy.³⁰

Extended x-ray-absorption fine-structure measurements at the Si K absorption edge were carried out at the double-crystal monochromator beamline of the Canadian synchrotron radiation facility at the Aladdin Synchrotron Radiation Center (SRC). The Aladdin storage ring of SRC was operated at 800 MeV and 200 mA . The absorption spectra were recorded by detecting the sample current, which is proportional to the x-ray absorption,³¹ as a function of the incident photon energy in the $(1780\text{--}2500)\text{-eV}$ range. To improve the signal-to-noise ratio, up to four spectra of each sample were recorded and summed.

Figure 1(a) shows the Si K edge x-ray-absorption raw spectra of $a\text{-Si}_x\text{C}_{1-x}\text{:H}$ films as a function of the film composition. When the composition is varied, one can qualitatively observe changes in both the near-edge absorption region and the extended fine-structure oscillatory part of the spectra. A specific study of the near edge x-ray-absorption region will be reported in a separate paper. Here we will focus on the EXAFS oscillations region (from about a few tens of eV above the absorption edge up to 2500-eV photon energy).

The EXAFS signal was extracted from the raw x-ray absorption spectrum and analyzed according to the procedure reported in Ref. 32. Basically, the data analysis procedure consists of (i) transforming the spectra from energy to K space with k^3 multiplication; (ii) subtracting the nonoscillatory background generated by fitting the data by a three equal-section cubic spline function, and thereby isolating the characteristic EXAFS oscillations of the absorption coefficient; (iii) Fourier-transforming the k^3 -weighted oscillations in R space to obtain the approximate radial position (noncorrected from the phase shift) of the coordination shells surrounding the Si absorbing atoms; (iv) sorting out and back transforming in the K space the peak corresponding to a given coordination shell. This yields the characteristic EXAFS oscillations originating from a chosen coordination shell; and, finally, (v) curve fitting of these characteristic oscillations with the known backscattering amplitudes and phase-shift functions of the individual components involved in a

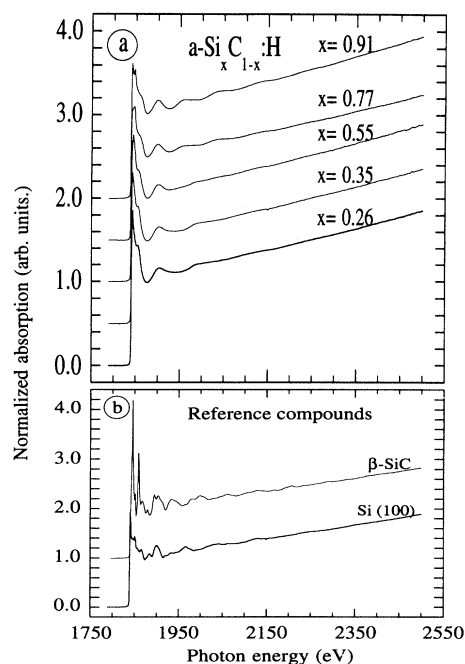


FIG. 1. Si K edge x-ray-absorption raw spectra (a) of $a\text{-Si}_x\text{C}_{1-x}\text{:H}$ films as a function of the film composition, and (b) of $\beta\text{-SiC}$ and $\text{Si}(100)$ single-crystal reference compounds. The spectra have been vertically displayed for convenience.

given environment; this allows the extraction of the quantitative structural parameters of the sorted out coordination shell. We have used a nonlinear least-square multfile based fitting procedure developed by Aebi *et al.*³² More details on the reliability, and the advantages of using this procedure are discussed in Ref. 32.

Single crystalline Si ($c\text{-Si}$) and silicon carbide ($\beta\text{-SiC}$) were used as reference compounds, as shown in Fig. 1(b), to extract the backscattering amplitude and the phase-shift function of the Si-Si and Si-C pairs of atoms, respectively. Prior to the measurement, the $\text{Si}(100)$ sample was cleaned using a HF-based recipe. The $\beta\text{-SiC}$ sample was analyzed as received. Figure 2 shows the radial distributions of the $c\text{-Si}$ and $\beta\text{-SiC}$ reference compounds. For $c\text{-Si}$ (100), the most prominent peak corresponds to the first coordination shell composed of four Si atoms located at 2.35 \AA (once the phase shift is taken into account). For $\beta\text{-SiC}$, the first-shell peak is due to the four C atoms located at 1.88 \AA . The second coordination shell of $\beta\text{-SiC}$ structure is composed of 12 Si atoms at a distance of 3.08 \AA .

From EXAFS analysis of $a\text{-Si}_x\text{C}_{1-x}\text{:H}$ films, the short-range-order around the Si atoms was characterized by determining the following structural parameters: (i) the interatomic distance ($R_{\text{Si-Si}}$ and $R_{\text{Si-C}}$); (ii) the partial coordination numbers ($N_{\text{Si-Si}}$ and $N_{\text{Si-C}}$, i.e., the number of Si and C atoms nearest neighbors of the silicon absorbing atoms, respectively); and (iii) the Debye-Waller factor or the mean-square relative displacements, along the absorber-backscatterer direction. These latter values are

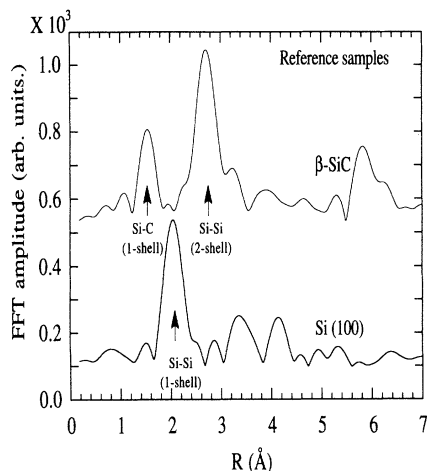


FIG. 2. Radial distribution functions of the k^3 -weighted EXAFS oscillations of the β -SiC and Si(100) reference compounds. Si-Si and Si-C pair first-shell contributions are indicated together with the Si-Si pair second coordination shell peak, in the case of β -SiC sample.

relative to the disorder factor in the reference compounds and will be noted $\Delta\sigma_{\text{Si-Si}}^2$ and $\Delta\sigma_{\text{Si-C}}^2$.

III. RESULTS AND DISCUSSIONS

A. Short-range-order changes as a function of the $a\text{-Si}_x\text{C}_{1-x}\text{:H}$ film composition

Figure 3 shows the Fourier transform of the k^3 -weighted EXAFS oscillations of the $a\text{-Si}_x\text{C}_{1-x}\text{:H}$ films with compositions varying from carbon-rich ($x=0.26$) to silicon-rich ($x=0.91$). From these radial structure functions, it is clearly observed that (i) only peaks corresponding to Si-C and Si-Si pair first-shell contributions are present (i.e., there are no significant peaks at higher radial positions) indicating a lack of long-range order in these alloys; and (ii) the Si-C and Si-Si peak components vary in opposite ways with the composition (x), i.e., Si-C peak gradually vanishes while Si-Si peak continuously grows when the film composition changes from carbon-rich to silicon-rich. One can note that for $x \geq 0.77$ compositions, the Si-C peak is embedded in the background oscillations and, consequently, cannot be extracted with confidence.

The first-shell peaks were treated as described in the previous section. The structural parameters obtained, as a function of the $a\text{-Si}_x\text{C}_{1-x}\text{:H}$ film composition, are summarized in Table I. Over all the investigated composition range ($x=0.26-0.91$), the average bond lengths of the Si-Si and Si-C bonds in the first coordination shell were found to be composition independent and equal to their crystalline values, namely, 2.35 and 1.88 Å, respectively. Similar results were reported by other authors in the case of $a\text{-Si}_x\text{C}_{1-x}\text{:H}$ alloys²⁴ or even $a\text{-Si}_x\text{Ge}_{1-x}\text{:H}$ alloys.³³ This behavior was interpreted as a consequence of the presence of structural disorder sufficient to allow the relaxation of the distances to their “molecular” values.^{11,24,33}

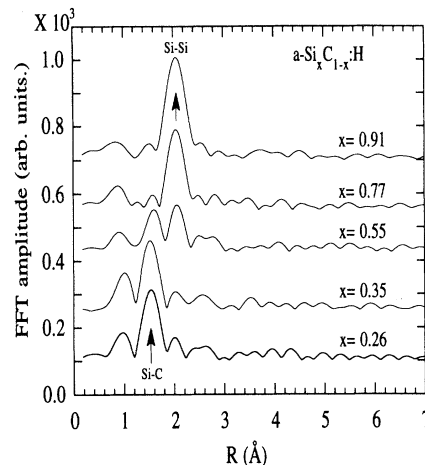


FIG. 3. Fourier-transform of the k^3 -weighted EXAFS oscillations of $a\text{-Si}_x\text{C}_{1-x}\text{:H}$ films as a function of the film composition. Peaks corresponding to the Si-C and Si-Si pair first-shell components are indicated.

The partial coordination numbers ($N_{\text{Si-Si}}$ and $N_{\text{Si-C}}$) provide an averaged picture of the local arrangements of the Si and C atoms, respectively, in the first coordination shell of the absorbing Si atoms. All the coordination numbers are normalized to 4, which is the total coordination number value found in the first coordination shell of the reference samples. Figure 4 shows the variation of $N_{\text{Si-C}}$ and $N_{\text{Si-Si}}$ as a function of the film composition. The investigated composition range can be divided in two parts. The first part ($0.26 \leq x \leq 0.55$) in which both Si-C and Si-Si pair components were extracted allowing to follow the arrangements of C and Si atoms in the local Si environments. In the second composition range ($x \geq 0.77$), only Si-Si environments related data were obtained from EXAFS analysis, due to both the low carbon content and the weak C backscattering cross section.

In the first composition range, the total coordination

TABLE I. The Si first coordination shell structural parameters of $a\text{-Si}_x\text{C}_{1-x}\text{:H}$ films as a function of the film composition. N , R , and $\Delta\sigma^2$ are the coordination number, the interatomic distance and the disorder factor for both Si-C and Si-Si pairs in the first coordination shell; *: reference samples; †: N_{Si} is the total coordination number of Si atoms, as seen by EXAFS ($N_{\text{Si}} = N_{\text{Si-Si}} + N_{\text{Si-C}}$). For the $x=0.77$ and 0.91 compositions, no Si-C bond contributions were observed by EXAFS.

Sample	Si-C			Si-Si			N_{Si}^\dagger
	$N_{\text{Si-C}}$	$R_{\text{Si-C}}$ (Å)	$\Delta\sigma_{\text{Si-C}}^2$ (10^{-3}Å^2)	$N_{\text{Si-Si}}$	$R_{\text{Si-Si}}$ (Å)	$\Delta\sigma_{\text{Si-Si}}^2$ (10^{-3}Å^2)	
$\beta\text{-SiC}^*$	1	1.88					
Si(100)*				1	2.35		
$a\text{-Si}_x\text{C}_{1-x}\text{:H}$							
$x=0.26$	0.83	1.88	0.99	0.12	2.36	1.7	0.95
$x=0.35$	0.75	1.88	0.33	0.18	2.38	7.0	0.93
$x=0.55$	0.47	1.89	1.20	0.26	2.37	0.44	0.73
$x=0.77$				0.56	2.36	1.2	
$x=0.91$				0.78	2.35	1.2	

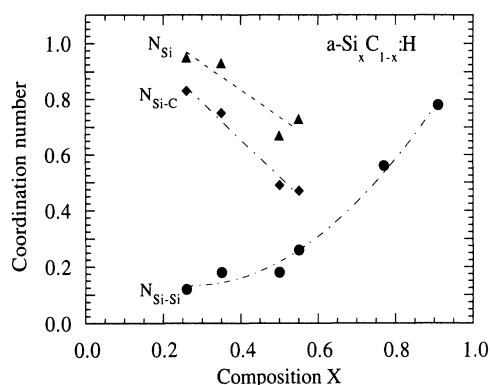


FIG. 4. Normalized partial ($N_{\text{Si-Si}}$ and $N_{\text{Si-C}}$) and total ($N_{\text{Si}} = N_{\text{Si-Si}} + N_{\text{Si-C}}$) coordination numbers of the Si first coordination shell, in $a\text{-Si}_x\text{C}_{1-x}\text{:H}$ films as a function of the film composition.

number (N_{Si}), seen by EXAFS, decreases from 0.95 to 0.73 when the composition is varied from $x = 0.26$ to 0.55 (see Fig. 4). The difference between the N_{Si} values and the maximum possible value of 1, is due to bonds not seen by EXAFS, namely, Si-dangling bonds and/or Si-H hydrogenated bonds. For the Si-H hydrogenated bond contribution, we have determined the Si-H bond densities of $a\text{-Si}_x\text{C}_{1-x}\text{:H}$ films by means of FTIR analysis. Figure 5 shows that the Si-H bond density of $a\text{-Si}_x\text{C}_{1-x}\text{:H}$ films increases when the silicon content is increased. By using these FTIR data, we calculated the ratio of Si-H hydrogenated bonds,³⁴ which is more appropriate for the comparison of the EXAFS and FTIR data. We found that for compositions $x = 0.26$, $x = 0.35$, and $x = 0.55$, 5.8%, 5.6% and 7.2% of the Si bonds are hydrogenated, respectively. Thus, for the C-rich compositions ($x = 0.26$ and 0.35), the proportion of Si bonds not seen by EXAFS (about 5% and 7%, respectively) is due to the Si-H bonds. This suggests that there is no significant proportion of Si dangling bonds in $a\text{-Si}_x\text{C}_{1-x}\text{:H}$ films at these C-rich compositions. For the $x = 0.55$ film composition, the EXAFS analysis yields a total coordination number (N_{Si}) of 0.73, and FTIR measurements show that about 7.2% of the Si bonds are hydrogenated at this film composition. The sum of both contributions shows that about 20% of the Si-X bonds (other than Si-C, Si-Si, and Si-H pairs) are still missing. This proportion is most likely due to Si dangling bonds.

On the other hand, in the $x = 0.26$ –0.55 composition range, Fig. 4 clearly shows that $N_{\text{Si-C}}$ decreases more rapidly than $N_{\text{Si-Si}}$ increases when the silicon content is increased. It is worth noting that by using the C-H bonds density data, provided by FTIR measurements, we deduced³⁵ that about 10% and up to 20% of C bonds are hydrogenated at $x = 0.26$ and 0.55 compositions, respectively. This significant increase of the C-H bond ratio, between $x = 0.26$ and 0.55 compositions, occurs to the detriment of Si-C bond formation contributing thereby to the observed variation of $N_{\text{Si-C}}$. Conversely, the slight increase of the Si-H bond ratio, observed in the $x = 0.26$ –0.55 composition range, contribute to the slow

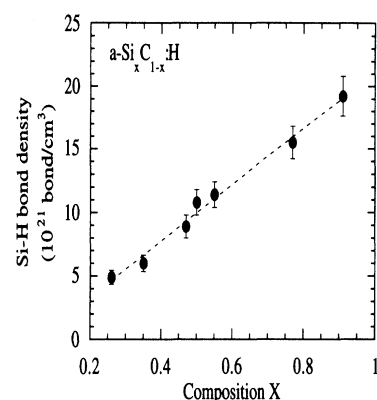


FIG. 5. Variation of the Si-H bond density with the $a\text{-Si}_x\text{C}_{1-x}\text{:H}$ film composition.

increase of $N_{\text{Si-Si}}$. This suggests that when the silicon content is increased from $x = 0.26$ to 0.55, only some of the C atoms are replaced by Si atoms in the local environments of Si atoms because of the incorporation of H atoms.

In the second composition range ($x = 0.77$ and $x = 0.91$), Fig. 4 shows a change in the slope of the $N_{\text{Si-Si}}$ variation curve, indicating a significant enrichment of the Si local environments in Si-Si pairs. Indeed, $N_{\text{Si-Si}}$ increases by about 40% while the average silicon content of the films is only increased by about 18% (from $x = 0.77$ to 0.91). For both $x = 0.77$ and 0.91 compositions, about 10% of Si bonds are hydrogenated. This suggests that the observed behavior of $N_{\text{Si-Si}}$ is most likely due to local chemical ordering that favors the formation of Si-rich local environments, as it will be discussed hereafter. A possible decrease of the Si dangling-bond ratio, when x varies from $x = 0.55$ to 0.91, would also contribute to the observed rapid increase of $N_{\text{Si-Si}}$.

In order to investigate the nature of the short-range ordering of Si environments in $a\text{-Si}_x\text{C}_{1-x}\text{:H}$ alloys, we compared the local carbon concentration, deduced from the ratio of partial coordination numbers [i.e., $N_{\text{Si-C}} / (N_{\text{Si-Si}} + N_{\text{Si-C}})$], to the average atomic carbon content, determined from the average Si/C atomic ratio measured by ERD. Figure 6 shows the local carbon concentration data as a function of the average atomic carbon concentration of $a\text{-Si}_x\text{C}_{1-x}\text{:H}$ alloys. In addition to the results of the present work, data from other works^{20,23,24} are also plotted on the same figure for comparison purposes. If the alloy is randomly disordered, the probability of finding C atoms as nearest neighbors of Si atoms would be proportional to the C atomic concentration.³³ From Fig. 6, it is clear that Si and C atoms in $a\text{-Si}_x\text{C}_{1-x}\text{:H}$ alloys are not randomly mixed, since all plots deviate from the line characterizing the random disorder. The other alternative for Si and C atom local arrangements is a complete chemical ordering. In this latter case, it is worth recalling the (i) nonmiscibility of Si and C atoms in the crystalline phase, and (ii) that the chemically ordered crystalline form only exists at the SiC

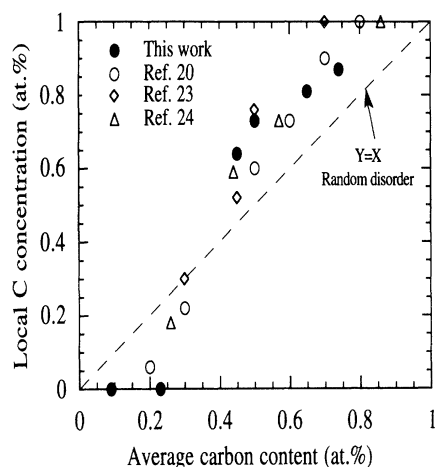


FIG. 6. The local carbon concentration around the Si atoms in the first coordination shell as a function of the average atomic content of carbon in the $a\text{-Si}_x\text{C}_{1-x}\text{:H}$ films. Other data from Refs. 20, 23, and 24 are also plotted for comparison.

stoichiometric ($x=0.5$) composition.^{11,24} Thus, for $a\text{-Si}_x\text{C}_{1-x}\text{:H}$ films at equiatomic proportions of Si and C ($x=0.5$), the complete local chemical ordering would correspond to a Si atom having only C atoms as nearest neighbors and would yield thereby a local carbon content of 100%. Figure 6 shows that, at $x=0.5$ composition, the local carbon content varies between 60% and 80% indicating that while $a\text{-SiC:H}$ alloys are not completely chemically ordered, nevertheless they exhibit a significant tendency for chemical ordering. One can also note that for atomic carbon contents higher than 70 at. %, the local carbon content is equal to 100%.^{20,23,24} This is due to the lower and lower silicon concentration in the alloy increasing thereby the probability for silicon atoms to be surrounded only by C atoms. Nevertheless, a chemical preference for Si-C bond formation might contribute to the attainment of such a high carbon content in the first-shell of Si atoms. For low atomic carbon contents (≤ 30 at. %), corresponding to Si-rich $a\text{-Si}_x\text{C}_{1-x}\text{:H}$ alloys, Fig. 6 shows that there is a preference for forming Si-Si bonds to the detriment of Si-C bonds. A quantitative analysis of the composition induced local order changes, based on a short-range-order coefficient calculations, will be presented in Sec. IV.

B. Short-range-order changes induced by thermal annealing of $a\text{-Si}_{0.5}\text{C}_{0.5}\text{:H}$ films

Since Si and C atoms are immiscible in the crystalline phase and the only chemically ordered form of the Si-C alloy exists at the stoichiometric composition, it is of particular interest, from the chemical-ordering tendency point of view, to study the effect of thermal annealings on the evolution of the microstructure of the amorphous stoichiometric $a\text{-Si}_{0.5}\text{C}_{0.5}\text{:H}$ ($a\text{-SiC:H}$) alloys, starting from the highly hydrogenated (≈ 30 at. %) as-deposited material and following the reorganization of the short-range order as the hydrogenated bonds (Si-H and C-H) are being dissociated in the annealed films.

As-deposited and annealed (550 °C, 650 °C, 750 °C, and

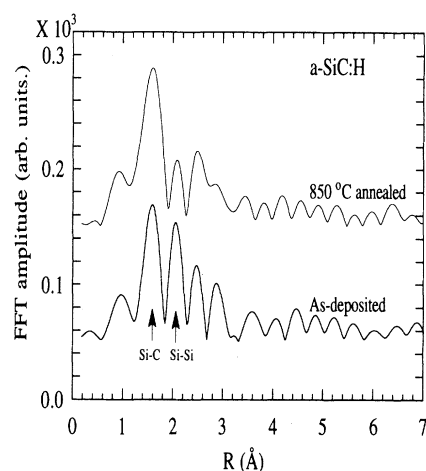


FIG. 7. Fourier-transform of the k^3 -weighted EXAFS oscillations of the as-deposited and the 850 °C annealed $a\text{-SiC:H}$ films.

850 °C) $a\text{-SiC:H}$ films were investigated. Figure 7 compares the Fourier transform of the k^3 -weighted EXAFS oscillations of the as-deposited and the 850 °C annealed films. It appears that when the $a\text{-SiC:H}$ film is annealed at 850 °C, the Si-C pair contribution increases, whereas the Si-Si pair contribution vanishes. To quantitatively follow the effect of thermal annealings on the short-range order, the Fourier-filtered first-shell EXAFS signals corresponding to the different annealing temperatures were fitted and the obtained structural parameters are reported in Table II.

From the as-deposited up to the 850 °C annealed $a\text{-SiC:H}$ samples, the interatomic distances ($R_{\text{Si-C}}$ and $R_{\text{Si-Si}}$) in the first shell do not show any significant variation and are nearly equal to their corresponding values in crystalline materials ($\beta\text{-SiC}$ and $c\text{-Si}$, respectively). This invariance of $R_{\text{Si-C}}$ and $R_{\text{Si-Si}}$ when the annealing temperature is increased up to 850 °C is most likely due to the presence of structural disorder.¹¹ Indeed, Zhang *et al.*¹³ have deduced from optical-absorption measurements of $a\text{-SiC:H}$ films that the hydrogen evacuation, under the effect of high temperature (400–950 °C) annealings, leads to an increase of the structural disorder.

The effect of thermal annealing on the reorganization of Si and C atoms in the first-shell can be followed

TABLE II. The first-shell structural parameters of $a\text{-SiC:H}$ films as a function of the annealing temperature.

$a\text{-SiC:H}$ Samples	Si-C			Si-Si			N_{Si}^{\dagger}
	$N_{\text{Si-C}}$	$R_{\text{Si-C}}$ (Å)	$\Delta\sigma_{\text{Si-C}}^2$ (10^{-3}Å^2)	$N_{\text{Si-Si}}$	$R_{\text{Si-Si}}$ (Å)	$\Delta\sigma_{\text{Si-Si}}^2$ (10^{-3}Å^2)	
As-deposited	0.49	1.89	1.90	0.18	2.35	0.67	0.67
Annealed at							
550 °C	0.49	1.89	1.00	0.16	2.36	0.75	0.65
650 °C	0.49	1.89	0.57	0.16	2.37	1.96	0.65
750 °C	0.84	1.90	5.40	0.11	2.38	1.80	0.95
850 °C	0.87	1.88	5.00	0.10	2.38	1.82	0.97

through the partial coordination numbers ($N_{\text{Si-C}}$ and $N_{\text{Si-Si}}$). Figure 8 shows the variation of $N_{\text{Si-Si}}$, $N_{\text{Si-C}}$, and N_{Si} ($N_{\text{Si}} = N_{\text{Si-Si}} + N_{\text{Si-C}}$) coordination numbers as a function of the annealing temperature. Two temperature ranges can be distinguished: (i) from as-deposited up to 650°C, $N_{\text{Si-C}}$ and $N_{\text{Si-Si}}$ remain constant; and (ii) for higher temperatures (650°C < $T \leq 850^\circ\text{C}$), $N_{\text{Si-Si}}$ slightly decreases, whereas $N_{\text{Si-C}}$ significantly increases. When the temperature is varied, N_{Si} abruptly increases from about 0.65 (for $T \leq 650^\circ\text{C}$) to around 0.95 (for $T \geq 750^\circ\text{C}$) as a consequence of a significant increase of the proportion of Si-C nearest-neighbor pairs in the first shell. The difference between N_{Si} and the maximum value of 1 is due to both the Si-H hydrogenated bonds and the Si-dangling bonds. At the 850°C annealing temperature, the N_{Si} value (0.97) suggests that the proportions of both Si-H and Si-dangling bonds are significantly reduced, as compared to the as-deposited *a*-SiC:H films.

Fourier-transform infrared measurements permit us to selectively follow the variation of the Si-H, C-H, and Si-C average bond densities as a function of the annealing temperature. Figure 9(a) clearly confirms that at $T > 650^\circ\text{C}$, a significant decrease of the hydrogenated bond (Si-H and C-H) densities occurs together with a substantial increase of the Si-C bond density. Indeed, Si-H bond density starts to decrease at temperatures higher than 500°C, whereas C-H bonds, more thermodynamically stable, abruptly dissociate at temperatures $\geq 650^\circ\text{C}$. Once both Si-H and C-H hydrogenated bonds are dissociated producing Si- and C-dangling bonds, the latter tend to recombine and additional Si-C bond formation takes place. From Si-H and C-H bond densities, and by using an average film density of 2.5 g/cm³, the bonded hydrogen content was estimated and plotted as a function of the annealing temperature [see Fig. 9(b)]. From the as-deposited up to the 500°C annealed films, where the hydrogenated bond average densities do not vary yet, the estimated bonded hydrogen content from FTIR measurements agrees with the total hydrogen content measured by ERD technique,¹² indicating that in the as-deposited

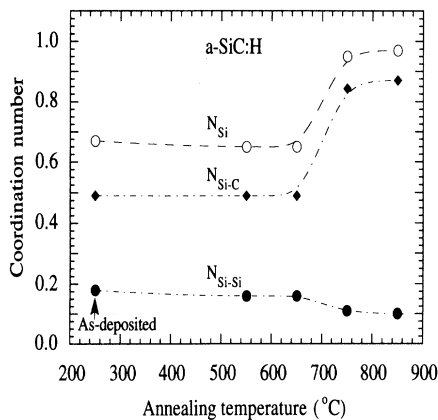


FIG. 8. Variation of the coordination numbers ($N_{\text{Si-Si}}$, $N_{\text{Si-C}}$, and N_{Si}) of the Si first coordination shell in *a*-SiC:H films as a function of the annealing temperature. The total coordination number N_{Si} is the sum of $N_{\text{Si-Si}}$ and $N_{\text{Si-C}}$.

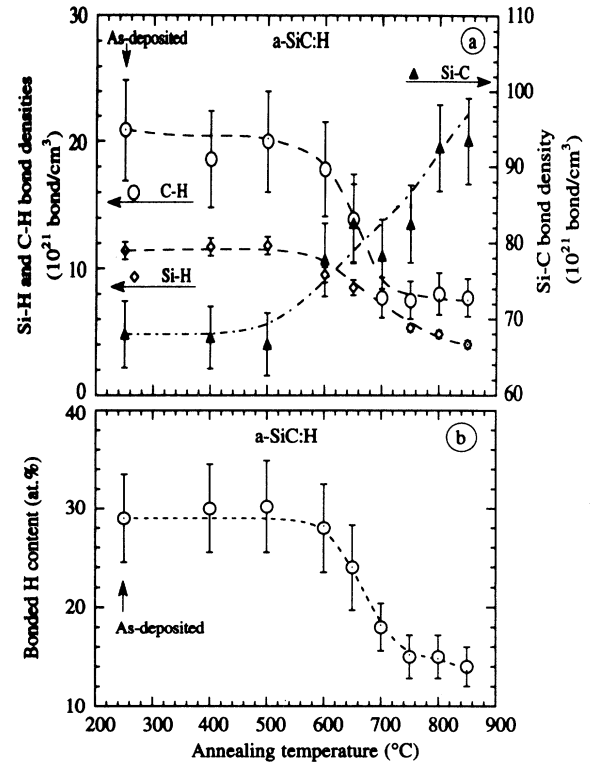


FIG. 9. Variation of the Si-H, C-H, and Si-C average bond densities (a), and of the bonded hydrogen content (b) of *a*-SiC:H films as a function of the annealing temperature.

a-SiC:H films all hydrogen atoms are bonded to either Si or C atoms. When the annealing temperature is varied between 600°C and 850°C, Fig. 9(b) clearly shows that the bonded hydrogen content of the *a*-SiC:H films decreases by about 55%.

By considering the N_{Si} value provided by EXAFS and the Si-H hydrogenated bonds ratio deduced from FTIR analysis, we estimated the proportion of Si-dangling bonds as a function of the annealing temperature. Figure 10 shows that the Si-dangling bonds ratio slightly increases from the as-deposited to the 650°C annealed films, and then rapidly decreases to reach zero at 850°C.

In summary, the microstructural changes produced by thermal annealings of *a*-SiC:H films, are (i) the significant dissociation of Si-H and C-H hydrogenated bonds leading to additional Si-C bonds formation (Fig. 9 and $N_{\text{Si-C}}$ in Fig. 8); (ii) the slight dissociation of Si-Si bonds ($N_{\text{Si-Si}}$ in Fig. 8); and (iii) the significant reduction of the proportion of the Si-dangling bonds (Fig. 10). These two latter points contribute also the observed increase of Si-C pairs in the Si first coordination shell. A quantitative analysis of these short-range-order changes, induced by thermal annealings, will be presented in Sec. IV.

C. Correlation between the stress of *a*-SiC:H films and their degree of structural disorder

The as-deposited *a*-SiC:H films are under high compressive stress (≈ -1 GPa). Their thermal annealing

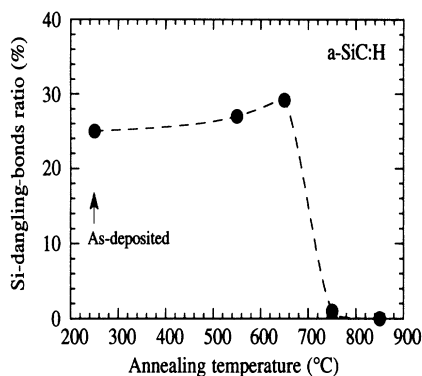


FIG. 10. The estimated Si-dangling bonds ratio of *a*-SiC:H films as a function of the annealing temperature.

induces a stress variation from compressive to tensile when the annealing temperature is varied from 300 °C to 850 °C. A nearly zero-stress and a high tensile stress ($\sim +1$ GPa) states are reached at 650 °C and 850 °C annealing temperatures, respectively.¹² This variation of the stress of *a*-SiC:H films is a consequence of the microstructural changes, induced by the annealing process.¹² So it is important to further understand the correlation between the stress of *a*-SiC:H films and their corresponding short-range-order characteristics.

In our *a*-SiC:H films, the disorder factors ($\Delta\sigma_{\text{Si-Si}}^2$ and $\Delta\sigma_{\text{Si-C}}^2$) provided by EXAFS analysis (see Table II) show that $\Delta\sigma_{\text{Si-Si}}^2$ remains nearly constant up to 550 °C and then increases to a nearly constant value over all the (650–850) °C temperature range. On the other hand, $\Delta\sigma_{\text{Si-C}}^2$ shows a more pronounced variation with a minimum value at $T=650$ °C (the temperature which corresponds to the nearly zero-stress state) and particularly high values for temperatures higher than 750 °C (corresponding to the high tensile stress states). The variation of $\Delta\sigma_{\text{Si-C}}^2$ as a function of the annealing temperature of *a*-SiC:H films is shown in Fig. 11. The $\Delta\sigma^2$ disorder factor is composed of two contributions, namely, the structural and the thermal components. Since we compare $\Delta\sigma_{\text{Si-C}}^2$ of the same Si-C pair at the same temperature (all the measurements were carried out at the room temperature), one can expect that the thermal component, as estimated by using a simple Einstein model,^{33,36} would be the same for all the samples. Consequently, the observed variation of $\Delta\sigma_{\text{Si-C}}^2$ mainly represents the variation of the structural component. This, in particular, shows that a nearly zero-stress state of *a*-SiC:H films corresponds to a minimum of structural disorder for the Si-C pair.

From FTIR analysis, we have also observed that when the annealing temperature is increased in the (300–850 °C) range, the Si-C stretching absorption band [peaking around (782 ± 4) cm^{-1} , for all samples] presents a minimum linewidth [full width at half maximum (FWHM)] value at 650 °C and broadens for the other temperatures, especially at annealing temperatures higher than 750 °C (see Fig. 11). This broadening of the Si-C absorption band is due to an enhancement of the bond angle distortions in the amorphous network.²⁸ Thus, both

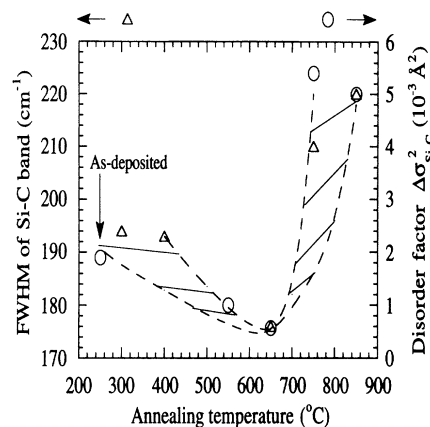


FIG. 11. Variation of both the disorder factor of the Si-C bonds ($\Delta\sigma_{\text{Si-C}}^2$ deduced from EXAFS data analysis) and the linewidth (FWHM) of the Si-C stretching absorption band (deduced from FTIR analysis) with the annealing temperature of *a*-SiC:H films.

EXAFS and FTIR measurements show that, from a structural viewpoint, the stress does not significantly affect the mean value of the Si-C bond lengths in the first shell, but seems to be more correlated to the degree of structural disorder in *a*-SiC:H films. This is in contrast to other systems such as Cu/Ni multilayers, where the thermal expansion mismatch between Cu and Ni does induce variations in the bond lengths and where EXAFS was used to determine the residual stresses for each layer respective of their elemental type (Cu or Ni)³⁷ (more details on either the interface sensitivity of EXAFS or the use of neutron diffraction method to investigate internal stresses in certain composite systems can be found in Refs. 37 and 38).

In summary, the dissociated C-H and Si-H bonds contribute to the compressive stress release through two mechanisms: either by (i) forming additional Si-C bonds and leading to a part of the initially bonded hydrogen atoms to be evacuated, or (ii) reforming other Si-H and C-H bonds under geometrical configurations allowing a minimization of the Si-C bond angle distortions in the amorphous network. An increase of the annealing temperature beyond 650 °C enhances both the hydrogenated bonds dissociation and the atom mobility which result in both: (i) a significant decrease of both the bonded hydrogen content and the Si-dangling bonds ratio, and (ii) a substantial increase of the Si-C bond density in the film. As a consequence of the rapid and random evacuation of the hydrogen atoms and the subsequent formation of the chemically favored Si-C bonds, the formed Si-C bonds are angularly distorted leading to an enhancement of the structural disorder in the annealed (≥ 750 °C) *a*-SiC:H films.¹³ The strengthening of the interaction among Si and C atoms in the amorphous network, through the formed Si-C bonds, leads to a film contracting and produces tensile stress.¹² This tensile stress does not affect the first-shell bond lengths, but seems to be accommodated through Si-C bond angle distortions.³⁹

IV. SHORT-RANGE-ORDER COEFFICIENT CALCULATIONS

A. The model

In order to quantify the observed tendency for nearest-neighbor chemical ordering in our $a\text{-Si}_x\text{C}_{1-x}\text{:H}$ alloys, we used the theoretical model developed by Cargill and Spaepen.²⁶ This model permits the characterization, in binary alloys, of departures from complete random disorder by calculating a short-range-order coefficient. In the case of $a\text{-SiC}$ alloys, this short-range-order coefficient ($\eta_{\text{Si-C}}^0$) can be written as follows:²⁶

$$\eta_{\text{Si-C}}^0 = \eta_{\text{Si-C}} / \eta_{\text{Si-C}}^{\text{max}} = [(N_{\text{Si-C}} / N_{\text{Si-C}}^*) - 1] / \eta_{\text{Si-C}}^{\text{max}}, \quad (1)$$

where (i) $N_{\text{Si-C}}$ is the partial coordination number of Si-C pairs, experimentally provided by EXAFS; (ii) $N_{\text{Si-C}}^*$ is the partial coordination number of Si-C pairs theoretically calculated in the case of a randomly disordered alloy; in the case of $a\text{-Si}_x\text{C}_{1-x}$ alloys, its value is given by²⁶

$$N_{\text{Si-C}}^* = (1-x)N_{\text{Si}}N_{\text{C}} / \langle N \rangle, \quad (2)$$

where N_{Si} and N_{C} represent the total coordination numbers for Si and C atoms, respectively, and $\langle N \rangle$ is the average coordination number defined as

$$\langle N \rangle = xN_{\text{Si}} + (1-x)N_{\text{C}} \quad (3)$$

and (iii) $\eta_{\text{Si-C}}^{\text{max}}$ is the maximum value which can be reached by $\eta_{\text{Si-C}}$. For $x \neq 0.5$, $\eta_{\text{Si-C}}^{\text{max}}$ can be calculated according to Eq. (4). For $x = 0.5$, $\eta_{\text{Si-C}}^{\text{max}}$ has to be deduced from Eq. (1) by introducing the maximum value of $N_{\text{Si-C}}$ (Ref. 26) (see Sec. VI C)

$$\begin{aligned} -\eta_{\text{Si-C}}^{\text{max}} &= (1-x)N_{\text{C}} / xN_{\text{Si}} \quad \text{for } (1-x)N_{\text{C}} < xN_{\text{Si}}, \\ -\eta_{\text{Si-C}}^{\text{max}} &= xN_{\text{Si}} / (1-x)N_{\text{C}} \quad \text{for } xN_{\text{Si}} < (1-x)N_{\text{C}}. \end{aligned} \quad (4)$$

Thus, the short-range-order coefficient ($\eta_{\text{Si-C}}^0$) permits the comparison of the ordering in $a\text{-Si}_x\text{C}_{1-x}$ alloys of different compositions. Indeed, it clearly appears from Eq. (1) that for a randomly disordered alloy, $\eta_{\text{Si-C}}^0$ (or $\eta_{\text{Si-C}}$) is equal to zero. Any departure from a random disorder towards a chemical ordering with chemical preference for Si-C nearest-neighbor pairs leads to a $\eta_{\text{Si-C}}^0 > 0$ positive value. Finally, $\eta_{\text{Si-C}}^0 < 0$ negative value denotes a departure from random disorder towards chemical clustering,²⁶ i.e., chemical tendency against Si-C bond formation.

Before calculating $\eta_{\text{Si-C}}^0$, we should recall that H atoms are also incorporated in our $a\text{-Si}_x\text{C}_{1-x}\text{:H}$ films, giving rise to Si-H and C-H bond formation and, consequently, affecting the total coordination numbers of Si and C atoms. Thus, to adapt this model originally developed for binary alloys to our (Si, C, H) ternary alloys, we dissociated the problem in two steps. We first take into account the hydrogen incorporation by estimating the ratios of Si-H and C-H bonds from FTIR and ERD data, as previously explained.^{34,35} This allows us the calculation of the effective total coordination number, that is the average number of nonhydrogen nearest neighbors (\tilde{N}_{Si} and \tilde{N}_{C} for Si and C atoms, respectively). The effective

coordination numbers were calculated according to

$$\tilde{N}_x = 1 - [X - H], \quad (5)$$

where $X \equiv \text{Si}$ or C , and $[X - H]$ represents the ratio of $X\text{-H}$ hydrogenated bonds. Second, we calculate the $\eta_{\text{Si-C}}^0$ by using the effective total coordination numbers (\tilde{N}_{Si} and \tilde{N}_{C} instead of $N_{\text{Si}} = N_{\text{C}} = 1$).

These effective total coordination numbers could be lowered further due to the presence of Si- and/or C-dangling bonds and/or to sp^2 hybridization of C atoms in the case of C-rich films. These two factors were not considered in this calculation, since we do not have any related quantitative data. Nevertheless any lowering of \tilde{N}_{Si} and/or \tilde{N}_{C} would yield higher values of $\eta_{\text{Si-C}}^0$, supporting even more the presence of chemical ordering (in the $0.26 \leq x \leq 0.55$ composition range). Moreover, in $a\text{-Si}_x\text{C}_{1-x}\text{:H}$ films, C atoms are mainly incorporated as methyl groups,^{18,40} reducing thereby the possibility of forming graphitic-type bonding.⁴¹ The probability of formation of sp^2 C bonds and/or having C-dangling bonds would increase with the carbon content. If we assume that about 20% of C bonds are under sp^2 hybridization and/or dangling bonds in C-rich films ($x = 0.26$ and 0.35), the corresponding values of $\eta_{\text{Si-C}}^0$ increase by about 10%. Similarly, if we consider that at $x = 0.55$ composition, there is about 20% of Si-dangling bonds the calculated value of $\eta_{\text{Si-C}}^0$ increases by about 20%, with respect to the case where the ratios of sp^2 bonding and/or dangling bonds were not considered. In the two following paragraphs, we will use this adapted model to characterize the short-range order of $a\text{-Si}_x\text{C}_{1-x}\text{:H}$ alloys in both cases: (i) as a function of the film composition, and (ii) as a function of the annealing temperature of $a\text{-SiC:H}$ films.

B. Film composition ($a\text{-Si}_x\text{C}_{1-x}\text{:H}$)

For each composition, the effective total coordination numbers (\tilde{N}_{Si} and \tilde{N}_{C}), the partial coordination number of Si-C pairs ($N_{\text{Si-C}}$ provided by EXAFS), and the calculated short-range-order coefficients ($\eta_{\text{Si-C}}$, $\eta_{\text{Si-C}}^{\text{max}}$, and $\eta_{\text{Si-C}}^0$) are reported in Table III. For the completely chemically-ordered $\beta\text{-SiC}$ reference material, the short-range-order coefficients present the maximum value of 1 (i.e., $\eta_{\text{Si-C}} = \eta_{\text{Si-C}}^{\text{max}} = \eta_{\text{Si-C}}^0 = 1$). Table III shows that for $a\text{-Si}_x\text{C}_{1-x}\text{:H}$ films in the ($0.26 \leq x \leq 0.55$) composition range, the normalized short-range coefficients ($\eta_{\text{Si-C}}^0$) present positive values, indicating a significant tendency for chemical preference for Si-C nearest-neighbor pairs. The $\eta_{\text{Si-C}}^0$ value increases from 0.31 to 0.57 when the carbon content is increased from 45 to 74 at. % ($x = 0.55$ to 0.26), suggesting an enhancement of the local chemical-ordering tendency in C-rich films. For both $x = 0.77$ and 0.91 Si-rich alloys, if a value of zero is used for $N_{\text{Si-C}}$ (no significant Si-C pair contribution was detected by EXAFS), highly negative values of $\eta_{\text{Si-C}}^0$ are yielded, suggesting a chemical preference that favors Si-Si nearest-neighbor pairs.

Both qualitative and quantitative analysis of the EXAFS data lead us to answer the short-range-order question, that is to say whether chemical ordering or ran-

TABLE III. Effective total coordination numbers and short-range-order coefficients of $a\text{-Si}_x\text{C}_{1-x}\text{:H}$ alloys at different compositions. \bar{N}_{Si} and \bar{N}_{C} are the effective total coordination numbers of Si and C atoms, respectively; $N_{\text{Si-C}}$ is the partial coordination number of Si-C pairs, provided by EXAFS; $\eta_{\text{Si-C}}^{\text{max}}$ and $\eta_{\text{Si-C}}^0$ are the maximum and the normalized value, respectively, of the calculated short-range-order coefficient ($\eta_{\text{Si-C}}$). For $x=0.91$, the C-H absorption band cannot be detected by FTIR due to the low C-H bond densities. Consequently, the corresponding \bar{N}_{C} value cannot be calculated.

Sample	\bar{N}_{Si}	\bar{N}_{C}	$N_{\text{Si-C}}$	$\eta_{\text{Si-C}}$	$\eta_{\text{Si-C}}^{\text{max}}$	$\eta_{\text{Si-C}}^0$
$a\text{-Si}_x\text{C}_{1-x}\text{:H}$						
$x=0.26$	0.94	0.90	0.83	0.21	0.37	0.57
$x=0.35$	0.94	0.89	0.75	0.25	0.57	0.44
$x=0.55$	0.93	0.80	0.47	0.22	0.70	0.31
$x=0.77$	0.91	0.88			0.29	
$x=0.91$	0.90					

dom disorder best describes the local environments of the Si atoms when the composition of the $a\text{-Si}_x\text{C}_{1-x}\text{:H}$ alloys is varied. Over all the investigated composition range, these alloys cannot be described as randomly disordered alloys. Indeed, two composition ranges can be distinguished: (i) for the ($0.26 \leq x \leq 0.55$) composition range, even if the values of $\eta_{\text{Si-C}}^0$ are still far from the maximum value of 1, there is a significant tendency for local chemical ordering, i.e., chemical preference for Si-C heteroatomic bonding. This chemical preference tendency increases with the carbon content. The incorporation of H atoms also influences the short-range-order since the proportion of Si-H and C-H hydrogenated bonds increases to the detriment of Si-Si and Si-C bond formation, when the silicon content is increased; and (ii) for the Si-rich $a\text{-Si}_x\text{C}_{1-x}\text{:H}$ alloys ($x \geq 0.77$), the obtained results suggest a presence of chemical clustering that favors the formation of the Si-Si bonds against the Si-C heteroatomic bondings in the local Si environments.

C. Thermal annealing of $a\text{-Si}_{0.5}\text{C}_{0.5}\text{:H}$

To calculate the $\eta_{\text{Si-C}}$ values, we used the quantitative data of Fig. 9(a), and estimated the effective total coordination numbers (\bar{N}_{Si} and \bar{N}_{C}), according to the same procedure explained above. In the case of $x=0.5$ composition, $\eta_{\text{Si-C}}^{\text{max}}$ is equal to 1 [by introducing $N_{\text{Si-C}}^{\text{max}}=1$, corresponding to $\beta\text{-SiC}$ crystalline material, in Eq. (1)]. Thus, $\eta_{\text{Si-C}}^0 = \eta_{\text{Si-C}}$ and the tendency for Si-C nearest-neighbor chemical ordering can be directly characterized by $\eta_{\text{Si-C}}$. The calculated values of $\eta_{\text{Si-C}}$ as a function of the annealing temperature of $a\text{-SiC:H}$ films are reported in Table IV.

For the as-deposited and the 550°C annealed $a\text{-SiC:H}$ films, $\eta_{\text{Si-C}}$ presents a value of 0.12 indicating the presence of a chemical preference for Si-C heteroatomic bonding. At 650°C annealing temperature, the $\eta_{\text{Si-C}}$ slightly decreases to a value of 0.07, suggesting a slight departure from a random disorder or a weak tendency for local chemical ordering. This could be the result of the annealing temperature which is likely not high enough to

TABLE IV. The effective total coordination numbers (\bar{N}_{Si} and \bar{N}_{C}) and the corresponding short-range-order coefficient ($\eta_{\text{Si-C}}$) of as-deposited and annealed $a\text{-SiC:H}$ films as a function of the annealing temperature. $N_{\text{Si-C}}$ is the partial coordination number of Si-C pairs, provided by EXAFS.

$a\text{-SiC:H}$ Samples	\bar{N}_{Si}	\bar{N}_{C}	$N_{\text{Si-C}}$	$\eta_{\text{Si-C}}$
As-deposited	0.92	0.85	0.49	0.12
Annealed at 550°C	0.92	0.86	0.49	0.12
650°C	0.94	0.90	0.49	0.07
750°C	0.96	0.95	0.84	0.75
850°C	0.97	0.95	0.87	0.81

produce a complete Si-C bond recombination of the created Si- and C-dangling bonds during the annealing (Fig. 10 shows that the maximum of the Si-dangling bonds ratio occurs at 650°C).

For temperatures higher than 650°C , the $\eta_{\text{Si-C}}$ presents high positive values, indicating that structural rearrangements occur with a strong local chemical ordering that favors the formation of Si-C heteroatomic bondings. As the temperature is increased, the $\eta_{\text{Si-C}}$ value approaches more and more the maximum value of 1 (corresponding to $\beta\text{-SiC}$), suggesting that the first-shell environments in the annealed ($T \geq 750^\circ\text{C}$) $a\text{-SiC:H}$ films evolve towards $\beta\text{-SiC}$ -like environments. If we extrapolate the $\eta_{\text{Si-C}}$ variation in the ($750\text{--}850^\circ\text{C}$) temperature range to higher temperatures, a complete chemical ordering ($\eta_{\text{Si-C}}=1$) would occur at about 1200°C annealing temperature. This prediction is consistent with the experimental results, since it has been observed that crystallization of $a\text{-SiC:H}$ PECVD films occurs at around 1200°C annealing temperature.⁴² At such high temperatures, it is worth mentioning that the tensile stress would be very high and could produce a film delamination, depending on the film thickness.

V. CONCLUSION

We have achieved both qualitative and quantitative characterizations of the short-range-order and the bonding states of amorphous hydrogenated silicon carbide films as a function of the film composition and the post-annealing temperature parameters. We were thus able (i) to determine the predominant form of the local ordering which best describes our $a\text{-Si}_x\text{C}_{1-x}\text{:H}$ films as a function of their composition or the post-annealing temperature; (ii) to determine the microstructural changes induced by thermal annealings of $a\text{-SiC:H}$ films; (iii) to point out the effect of hydrogenated bonds on both the composition-induced local disorder and the stress of the $a\text{-Si}_x\text{C}_{1-x}\text{:H}$ films; and (iv) to correlate the thermal-annealing-induced stress variation of $a\text{-SiC:H}$ films with both their bonding state changes and their degree of structural disorder.

Regarding the composition related local disorder, we have shown that over all the investigated composition range ($0.26 \leq x \leq 0.91$), $a\text{-Si}_x\text{C}_{1-x}\text{:H}$ alloys cannot be described as randomly disordered alloys. Two main composition ranges with different predominant forms of local ordering were identified: (i) the $0.26 \leq x \leq 0.55$ composi-

tion range, where the $a\text{-Si}_x\text{C}_{1-x}\text{:H}$ alloys exhibit a significant tendency for local chemical ordering. This tendency for chemical preference for Si-C nearest-neighbor pairs was found to increase when the carbon content is increased; and (ii) the Si-rich ($x \geq 0.77$) composition range, where the short-range-order was found to be characterized by chemical clustering that promotes the formation of Si-Si nearest-neighbor pairs against heteroatomic Si-C bonding, in the Si local environments.

For the thermal-annealing-induced local ordering changes, we have shown that the annealing of $a\text{-SiC:H}$ films from 300 °C to 850 °C temperatures produces microstructural changes together with a strong stress variation. In particular, we have pointed out that this stress variation is correlated to the (Si-H, C-H, and Si-C) bond densities variations and to the degree of structural disorder. Indeed, it is shown that at 650 °C, the compressive stress relaxation is caused by the hydrogenated bond dissociation leading, on one hand, to the formation of a fraction of Si-C bonds and thereby to the evacuation of some hydrogen atoms and, on the other hand, to the redistribution of H atoms to reform Si-H and C-H bonds under

configurations which minimize Si-C bonds angle distortions (the Si-Si and Si-C bond lengths in the first coordination shell were found to be stress independent). Beyond 650 °C, the hydrogen atom evacuation, the dangling bonds reduction, and the additional Si-C bonds formation are thermally enhanced, increasing thereby the structural disorder. The formation of Si-C bonds is favored by the strong chemical preference for Si-C nearest-neighbor pairs (highly positive $\eta_{\text{Si-C}}$ values) in the first coordination shell of Si atoms. Thus, when the annealing temperature is increased ($T > 650$ °C), the tensile stress in $a\text{-SiC:H}$ films increases, as a consequence of the additional formation of Si-C bonds.

ACKNOWLEDGMENTS

We would like to thank Dr. S.C. Gujrathi, from Université de Montréal, for the ERD analysis. This work was supported by the NSERC of Canada in the framework of MICRONET (Center of excellence on microelectronic devices, circuits, and systems for ULSI).

- ¹J. Bullo and M. P. Schmidt, *Phys. Status Solidi B* **143**, 345 (1987).
- ²M. P. Schmidt, I. Solomon, H. Tran-Quoc, and J. Bullo, *J. Non-Cryst. Solids* **77/78**, 849 (1985).
- ³A. H. Mahan, D. L. Williamson, M. Ruth, and P. Raboisson, *J. Non-Cryst. Solids* **77/78**, 861 (1985).
- ⁴A. Catalano, J. Newton, M. Trafford, and A. Rothwarf, *IEEE Trans. Electron. Devices* **ED-36**, 2839 (1989).
- ⁵J. W. Edington, D. L. Rowcliffe, and J. L. Henshall, *Powder Metall. Int.* **7**, 82 (1975); **7**, 136 (1975).
- ⁶A. Bolz and M. Schaldach, in *Proceedings of the Annual International Conference of the IEEE Engineering in Medicine and Biology Society, Seattle, 1989*, edited by Y. Kim and F. A. Spelman (IEEE, New York, 1989), Vol. 1, p. 164.
- ⁷A. R. Shimkunas, P. E. Mauger, L. P. Bourget, R. S. Post, L. Smith, R. F. Davis, G. M. Wells, F. Cerrina, and R. B. McIntosh, *J. Vac. Sci. Technol. B* **9**, 3258 (1991).
- ⁸M. Chaker, S. Boily, Y. Diawara, M. A. El Khakani, E. Gat, A. Jean, H. Lafontaine, H. Pépin, J. Voyer, J. C. Kieffer, A. M. Haghiri-Gosnet, F. R. Ladan, M. F. Ravet, Y. Chen, and F. Rousseaux, *J. Vac. Sci. Technol. B* **10**, 3191 (1992).
- ⁹M. A. Petrich, K. K. Gleason, and J. A. Reimer, *Phys. Rev. B* **36**, 9722 (1987).
- ¹⁰A. Jean, M. A. El Khakani, M. Chaker, S. Boily, E. Gat, J. C. Kieffer, H. Pépin, M. F. Ravet, and F. Rousseaux, *Appl. Phys. Lett.* **62**, 2200 (1993).
- ¹¹S. R. Elliott, *Adv. Phys.* **38**, 1 (1989).
- ¹²M. A. El Khakani, M. Chaker, A. Jean, S. Boily, H. Pépin, J. C. Kieffer, and S. C. Gujrathi, *J. Appl. Phys.* **74**, 2834 (1993).
- ¹³F. Zhang, H. Xue, Z. Song, Y. Guo, and G. Chen, *Phys. Rev. B* **46**, 4590 (1992).
- ¹⁴H. Wieder, M. Cardona, and C. R. Guarnieri, *Phys. Status Solidi B* **92**, 99 (1979).
- ¹⁵Y. Catherine and G. Turban, *Thin Solid Films* **70**, 101 (1980).
- ¹⁶K. Mui, D. K. Basa, and F. W. Smith, *Phys. Rev. B* **35**, 8089 (1987).
- ¹⁷I. Solomon, M. P. Schmidt, C. Senemaud, and M. D. Khodja, *Phys. Rev. B* **38**, 13 263 (1988).
- ¹⁸E. Gat, M. A. El Khakani, M. Chaker, A. Jean, S. Boily, H. Pépin, J. C. Kieffer, J. Durand, B. Cros, F. Rousseaux, and S. Gujrathi, *J. Mater. Res.* **7**, 2478 (1992).
- ¹⁹I. Solomon, M. P. Schmidt, and H. Tran-Quoc, *Phys. Rev. B* **38**, 9895 (1988).
- ²⁰A. Filipponi, P. Fiorini, F. Evangelisti, A. Balerna, and S. Mobilio, *J. Phys. (Paris) Colloq.* **47**, C8-357 (1986).
- ²¹S. Mobilio and A. Filipponi, *J. Non-Cryst. Solids* **97&98**, 365 (1987).
- ²²C. Meneghini, S. Pascarelli, F. Boscherini, S. Mobilio, and F. Evangelisti, *J. Non-Cryst. Solids* **137&138**, 75 (1991).
- ²³A. M. Haghiri-Gosnet, F. Rousseaux, E. Gat, J. Durand, and A. M. Flank, *Microelectron. Eng.* **17**, 215 (1992).
- ²⁴S. Pascarelli, F. Boscherini, S. Mobilio, and F. Evangelisti, *Phys. Rev. B* **45**, 1650 (1992).
- ²⁵F. Finocchi, G. Galli, M. Parrinello, and C. M. Bertoni, *Phys. Rev. Lett.* **68**(20), 3044 (1992).
- ²⁶G. S. Cargill III and F. Spaepen, *J. Non-Cryst. Solids* **43**, 91 (1981).
- ²⁷A. Jean, M. Chaker, Y. Diawara, P. K. Leung, E. Gat, P. P. Mercier, H. Pépin, S. Gujrathi, G. G. Ross, and J. C. Kieffer, *J. Appl. Phys.* **72**, 3110 (1992).
- ²⁸D. K. Basa and F. W. Smith, *Thin Solid Films* **192**, 121 (1990).
- ²⁹A. A. Langford, M. L. Fleet, B. P. Nelson, W. A. Langford, and N. Maley, *Phys. Rev. B* **45**, 13 367 (1992).
- ³⁰S. C. Gujrathi, P. Aubry, L. Lemay, and J. P. Martin, *Can. J. Phys.* **65**, 950 (1987).
- ³¹C. E. Bouldin, R. A. Forman, and M. I. Bell, *Phys. Rev. B* **35**, 1429 (1987).
- ³²P. Aebi, T. Tyliczszak, A. P. Hitchcock, K. M. Baines, T. K. Sham, T. E. Jackman, J. M. Baribeau, and D. J. Lockwood, *Phys. Rev. B* **45**, 13 579 (1992).
- ³³L. Incoccia, S. Mobilio, M. G. Proietti, P. Fiorini, C. Giovannella, and F. Evangelisti, *Phys. Rev. B* **31**, 1028 (1985).
- ³⁴Since the density and the hydrogen content of $a\text{-Si}_x\text{C}_{1-x}\text{:H}$ films vary with the film composition (Ref. 27), one has to nor-

malize the Si-H bond density to the total possible Si bond density. Thus, for each composition, by using the film density (g/cm^3), the precise atomic film composition (Si, C, and H content in at. %), and the maximum coordinance of 4 for Si atoms, the total possible Si-X bond density ($X \equiv \text{Si, C, or H}$) was estimated. Then, the proportion of Si-H hydrogenated bonds, with respect to the total Si-X bonds, was calculated using the Si-H bond density data, reported in Fig. 5.

³⁵We calculated the proportion of C-H bonds, with respect to the total C-X bonds ($X \equiv \text{Si, C, or H}$) following the same procedure used for the Si-H bonds ratio estimation (Ref. 34). In this case, we assumed a maximum coordination number of 4 for C atoms; lower C coordination numbers, due to the presence of C atoms under sp^2 hybridization, would yield higher C-H bonds ratios. Our estimations of the hydrogenated bonds ratios are comparable with the data reported by Mui, Basa, and Smith (Ref. 16).

³⁶A. Filipponi, D. Della Sala, F. Evangelisti, A. Balerna, and S.

Mobilio, *J. Phys. (Paris) Colloq.* **47**, C8-375 (1986).

³⁷E. V. Barrera, in *Residual Stresses in Composites: Measurements Modeling and Effects on Thermo-Mechanical Behavior*, edited by E. V. Barrera and I. Dutta (The Minerals, Metals, and Materials Society, Warrendale, PA, 1993), pp. 79–94.

³⁸R. I. Todd and B. Derby, in *Residual Stresses in Composites: Measurements Modeling and Effects on Thermo-Mechanical Behavior*, edited by E. V. Barrera and I. Dutta (The Minerals, Metals, and Materials Society, Warrendale, PA, 1993), pp. 147–160.

³⁹J. C. Woicik, C. E. Bouldin, J. O. Cross, L. B. Sorensen, and C. A. King, *J. Vac. Sci. Technol. B* **9**, 2194 (1991).

⁴⁰J. Sotiropoulos and G. Weiser, *J. Non-Cryst. Solids* **97&98**, 1087 (1987).

⁴¹A. H. Mahan, B. von Roedern, D. L. Williamson, and A. Madan, *J. Appl. Phys.* **57**, 2717 (1985).

⁴²B. Ruttensperger, G. Krötz, G. Müller, G. Derst, and S. Kalbitzer, *J. Non-Cryst. Solids* **137&138**, 635 (1991).